



Development of an Experimental Device for the Assessment of Emulsions Dynamic Behavior and Stability in Micro-gravity

Angeliki P. Chondrou¹ · Sotiris P. Evgenidis¹ · Konstantinos A. Zacharias^{1,2} · Margaritis Kostoglou¹ · Thodoris D. Karapantsios¹

Received: 16 March 2023 / Accepted: 15 May 2023
© The Author(s), under exclusive licence to Springer Nature B.V. 2023

Abstract

Emulsions are encountered in foods, cosmetics and pharmaceuticals. Their stability depends strongly on gravity (creaming or sedimentation) and interface driven destabilization mechanisms (coalescence or aggregation) occurring after their production. Although of great significance, coalescence and aggregation cannot be studied in-depth on ground due to coupling with gravity driven mechanisms. To overcome this restriction, the design, development and preliminary testing of a new experimental device to be used in the forthcoming ESA parabolic flights for the evaluation of emulsion dynamic behavior and stability under low gravity conditions, is presented. Such conditions allow to get rid of creaming and sedimentation and, thus, to isolate droplets coalescence and aggregation. A novel miniature emulsification cell, along with advanced electrical and optical diagnostics to produce and investigate emulsions are incorporated to custom experimental cells. Optical diagnostics include a high speed camera (up to 750.000 fps) to monitor droplets breakup and droplet-droplet interactions and a high resolution DSLR camera (20MP) to determine droplet size distribution. The EU patented I-VED electrical impedance spectroscopy technique (*EP 3 005 942 A1, 2016*) is employed to monitor the evolution of oil volumetric fraction as a function of time and gravity. Experimental parameters under study include: oil volume fraction, surfactant concentration, pulsation duration and stroke frequency for emulsification. The implementation of the experimental device, including two racks and one baseplate, complies with ESA technical requirements and safety regulations, while a number of experiments on-ground with a conventional oil-in-water emulsion validates it from a technical and functional point of view.

Keywords Emulsion stability · Micro-gravity · Droplets interactions · Coalescence · Electrical impedance spectroscopy · High-speed imaging

Introduction

Emulsions are systems consisting of two immiscible liquids, where droplets of the first liquid (dispersed phase) are dispersed within the second liquid (continuous phase) (Lorusso et al. 2021). Based on the type of the dispersed and continuous phase, they can be divided into three categories: a)

water-in-oil (W/O) emulsions, b) oil-in-water (O/W) emulsions and c) multiple emulsions that can be considered as emulsions of emulsions (W/O/W or O/W/O) (Akbari et al. 2018). Emulsions are encountered in foods (i.e. mayonnaise, salad creams and deserts), cosmetics (i.e. hand creams, lotions and hair sprays) and pharmaceuticals. They are also involved in almost every step of oil industry, from crude oil extraction to the final combustion of fuels in cars and thermoelectric plants (Chappat 1994).

Mixing of two immiscible liquids aiming to produce an emulsion results to a thermodynamically unstable system because of the unfavorable contact between the organic (oil) and the aqueous phase. Therefore, the addition of a third component is necessary to stabilize the emulsion, called emulsifier. Surfactants, polymers, solid particles and blends are commonly used as emulsifiers and their role is to enhance the mechanical stability of the droplets

✉ Thodoris D. Karapantsios
karapant@chem.auth.gr

¹ Department of Chemical Technology and Industrial Chemistry, School of Chemistry, Aristotle University of Thessaloniki, University, Box 116, 541 24 Thessaloniki, Greece

² Hellenic Institute of Metrology, National Quality Infrastructure System, Block 45, 57022 Sindos, Thessaloniki, Greece

by forming layers at their surface (Tadros 2013). Emulsification is a dynamic and non-spontaneous process. Thus, there is a need for energy consumption to produce the droplets. In direct emulsification, the emulsifier is first dissolved into the phase where it is more soluble, the second phase is then added and, finally, the two phases are mixed together. High-pressure homogenizers, rotor-stator devices, ultrasound generators, membranes and micro-channels are commonly applied to produce a dispersion of droplets with the aid of the proper type and concentration of emulsifier. Among these techniques, rotor-stator devices are considered the most suitable ones. They ensure high shear mixing of the two phases that succeeds the deformation of droplets that is necessary to break up a droplet into smaller ones (Leal-Calderon et al. 2007; Schramm 2005).

Emulsion stability, either wanted or unwanted, is critical for all applications and can be affected by different factors: a) *Droplet size distribution*: The emulsion becomes more stable for narrower droplet size distribution, b) *Dispersed phase volume fraction*: As volume of dispersed phase increases, the interfacial film progressively expands to surround the droplets and, thus, emulsion stability decreases, c) *Bulk viscosity of continuous phase*: Increase of viscosity reduces the collision frequency and the coalescence rate of droplets, resulting in more stable emulsions (Rosen 2004). Furthermore, emulsion stability strongly depends on different destabilization mechanisms that may take place as soon as produced water-in-oil or oil-in-water emulsions are stored in vessels and left still, with creaming (separation of emulsion into the dense and the dilute part), sedimentation (due to the difference in water and oil density), coalescence (due to thinning and disruption of the liquid film between droplets), aggregation (formation of accumulated droplets) and Ostwald ripening (disproportionation due to finite solubility of the liquids) being the most important among them (Varka et al. 2011). A schematic representation of the destabilization mechanisms is presented in Fig. 1.

After the end of the emulsification process, creaming or sedimentation takes place and, as a consequence, two different phases coexist in the test vessel: the creamy and the aqueous one. Typically, these two phases constitute an emulsion since they both contain water and oil but at different proportions. Phase separation due to aforementioned gravity driven processes makes droplets come in close contact and, then, two interface driven processes (coalescence and aggregation) are rapidly evolving. These processes increase the size of droplets and may lead eventually to the complete separation of the system into the two immiscible bulk liquids. Although of great importance for emulsion stability, coalescence and aggregation cannot be studied thoroughly and independently due to their rapid evolution and coupling with gravity driven ones.

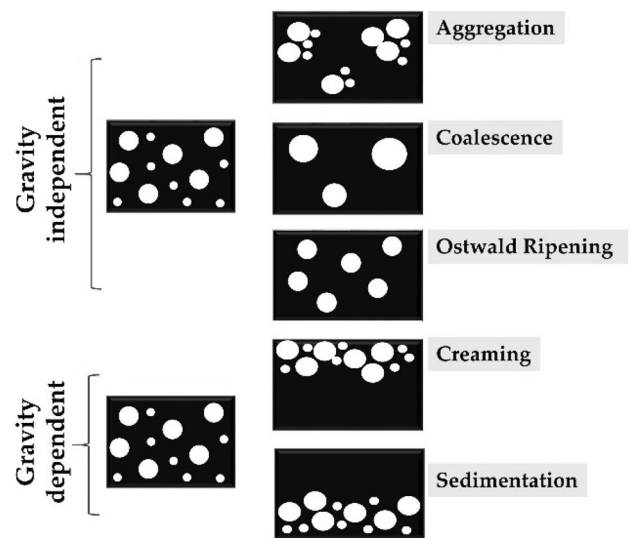


Fig. 1 Emulsion destabilization mechanisms

Emulsion stability is usually assessed in literature by optical techniques (i.e. microscopy, static light scattering and diffusing wave spectroscopy), electrical techniques (i.e. electrical pulse counting) and electroacoustic techniques (i.e. ultrasonic, dielectric spectroscopy). Apart from these, another simple and non-intrusive technique, electrical impedance spectroscopy which employs electrical measurements to estimate dispersed phase fraction is used. This technique is based on the electrical resistance change of the emulsion during phase separation due to the conductivity difference of the two phases (water is conductive while oil droplets are non-conductive) (McClements 2005; Vlachou et al. 2020).

This work aims to investigate solely the rapid interface driven emulsion destabilization mechanisms. To do this, as mentioned above, the respective gravity driven mechanisms have to be eliminated and this can be achieved in a low gravity environment. Here, we develop an experimental setup to be used in the forthcoming European Space Agency (ESA) Parabolic Flight Campaigns (PFCs), where evolved low gravity conditions will be exploited to study the two interface driven processes that evolve quickly (coalescence and aggregation). In the absence of gravity period during each parabola (20–22 seconds), buoyancy related phenomena are eliminated. This means that the gravity driven processes of creaming and sedimentation will not appear after the end of the emulsification and, thus, the two phases (creamy and aqueous) will not separate. It is noticed that the focus here is to observe phenomena occurring after emulsification since the effect of gravity on emulsification appears to be quite limited. The emulsification itself is a quite complex process including droplet deformation, coalescence and/or breakage in the highly sheared domain between piston and

cell (Chondrou et al. 2021; Guido and Simeone 1998; Liu et al. 2018). The only relevance of the emulsification here is the production of the droplet size distribution to be studied under microgravity and hypergravity conditions. Consequently, droplet-droplet interactions after emulsification, due to interface driven processes will happen slower and independently of the gravity driven ones. Therefore, motion and coalescence/aggregation of droplets can be monitored by means of advanced diagnostics, enabling better understanding of underlying phenomena that cannot be captured under terrestrial conditions. The design and implementation of the experimental device complying with ESA requirements, accompanied with preliminary (ground) experimental results are presented hereafter.

Materials and Methods

Device Description

The experimental device is divided into three parts, two experiment racks and one separate baseplate (Fig. 2), for two reasons: a) its total weight cannot exceed 200 kg and b) to facilitate its use during the experiments under microgravity conditions. Each rack is composed of the primary structure and the payload. The primary structure consists of a machined aluminum plate as well as different Rexroth Bosch® items and connecting elements. Proper perpendicular and horizontal profiles are fastened together with brackets to form the desired structure, which is then fixed on the plate with brackets as well. The payload added to the primary structure includes scientific equipment, custom parts or units, laptops and extra strut profiles. For the needs of experiments under micro-gravity conditions, the plate of

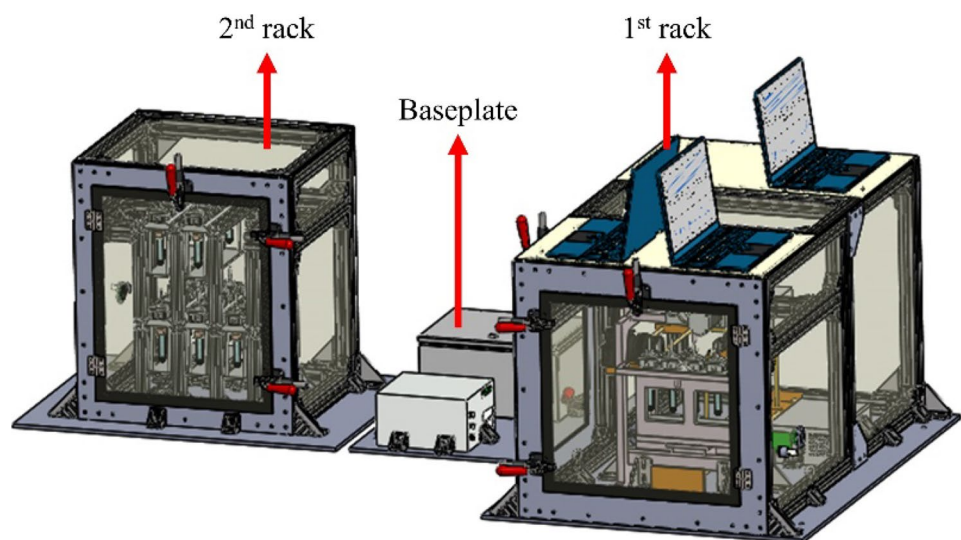
each rack is screwed to the fixation system of the aircraft that performs the parabolic flights.

The dimensions of 1st rack's primary structure are 123 x 67 x 70 cm and its payload consists of the emulsification unit, the optical and electrical diagnostics. The corresponding dimensions for the 2nd rack are 43 x 40 x 70 cm, while its payload includes the storage unit for 30 experimental cells. Polycarbonate sheets surround each experiment rack for the protection of the operators and preventing any liquid leakage as well. The 1st and the 2nd rack are equipped with two and one access doors, respectively. The baseplate is used to secure the electrical control panel of the device and the processor of the high-speed camera applied to capture droplets interactions (dimensions: 54 x 73 x 1 cm). In the following subsections a more detailed description of both racks and baseplate is presented.

1st Rack

The emulsification unit, Fig. 3b, constitutes the core of the 1st rack (Fig. 3a). It is similar to the miniature pulsating emulsification device used on-ground by (Chondrou et al. 2020, 2021). This unit consists of the aluminum frame, the motor unit and the case that supports five identical experimental cells (Fig. 3b). Both motor unit and cell case are integrated in the metallic frame of the emulsification unit. The motor unit which is utilized to drive a piston that mixes the two phases and also produces, deforms and breaks up droplets during emulsification, includes the stepper motor (NEMA 23, 23HD86001Y-21B, step angle 1.8°, holding torque 280 N.cm) and the rack-pinion gear system (Fig. 3c). On the other hand, the cell case (Fig. 4a) is placed on a carrier that facilitates its displacement at five fixed positions to use a different experimental cell in each parabola of a 5-parabolas sequence (Fig. 4b).

Fig. 2 3D schematic representation of the experimental device



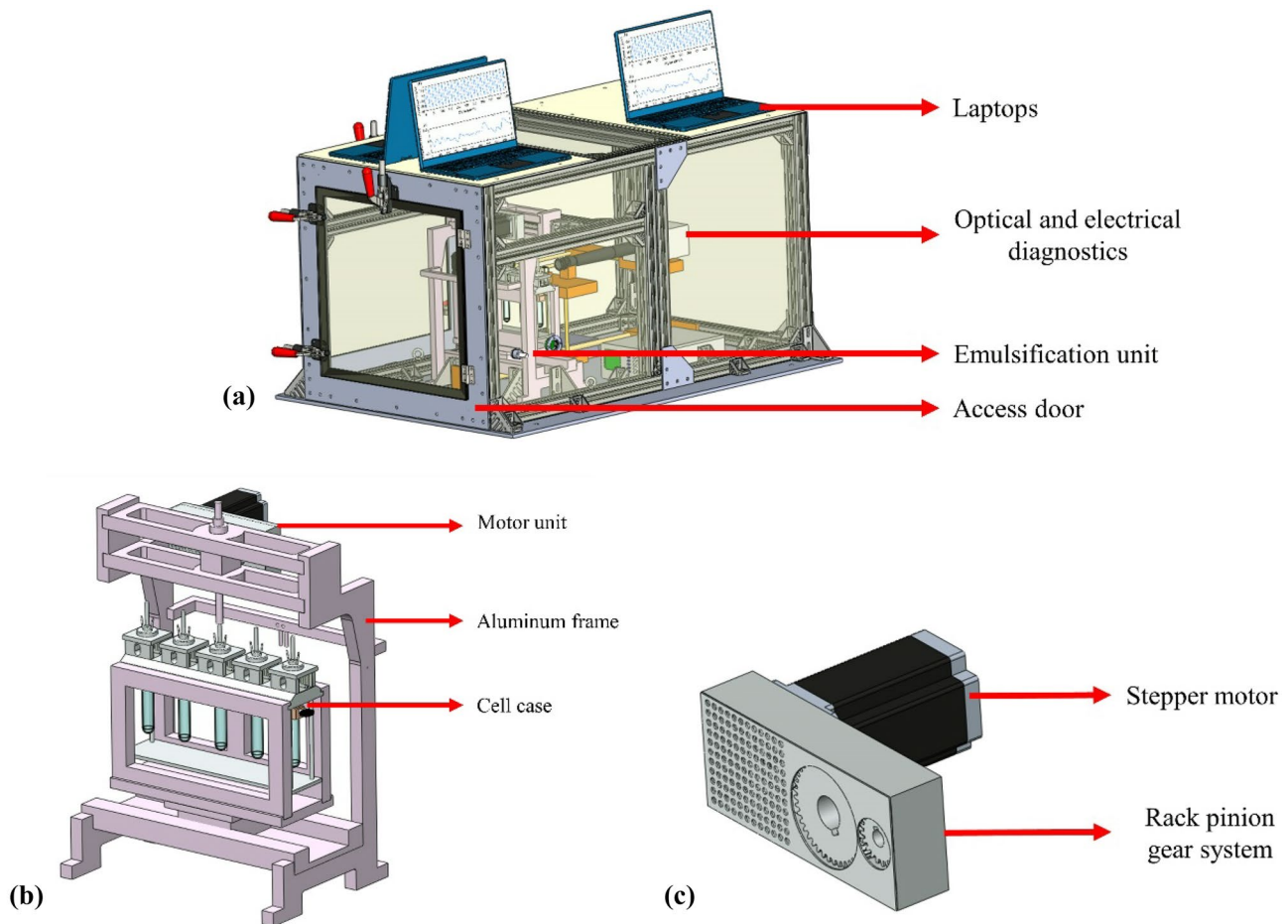


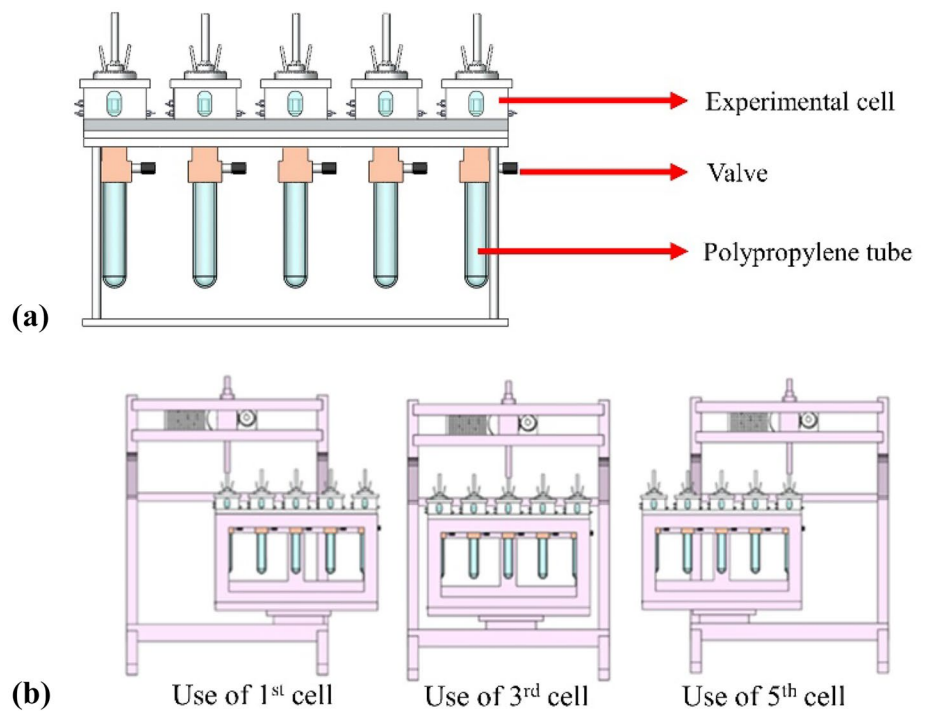
Fig. 3 **a** The 1st rack of experimental device, **b** The emulsification unit of the 1st experiment rack and **c** The motor unit of the emulsification unit

The experimental cell, inside which the emulsification process and the consequent study of emulsions' dynamic behavior and stability take place, is made mainly by aluminum. Its dimensions are 12 x 14 x 26 mm (Fig. 4c) and the total volume of the added liquids inside the cell cannot exceed 4 mL. Two of the parallel cell walls are made of glass offering ports for optical recordings and lighting. The two remaining walls are made of Plexiglas. Non-intrusive, rod electrodes are flush-mounted to the parallel Plexiglas walls for performing electrical measurements. A cylindrical piston is integrated to the lid of the cell. The tip of the piston ends to a thin aluminum, orthogonal plate which covers almost the entire cross section of the cell. Its height is 1.62 mm, while the gap between the plate and the cell walls is 0.66 mm. During emulsification, the piston moves continuously up and down along the perpendicular axis, scavenging the total internal volume of the cell. The piston motion is triggered by the stepper motor through the rack-pinion gear system that converts its rotary movement to the linear motion of the piston. Such a piston is employed in the FOAM-C cell,

a European Space Agency instrument designed and constructed for emulsification experiments onboard the International Space Station (ISS). The two pistons have the same shape and dimensions however they differ in the motion type. The present piston follows a sinusoidal type of motion while the FOAM-C piston follows a square wave motion (Born et al. 2021). To enable comparison with the results to be obtained from micro-gravity experiments during parabolic flights, the performance of this piston has already been examined under terrestrial conditions (Chondrou et al. 2020, 2021). The lid of the cell has also two communication ports for the addition of the liquids inside the cell. The bottom of the cell is connected with a polypropylene (PP) tube through a valve. When this valve opens, the produced emulsion can be collected in the PP tube that contains already a few mL of a dense surfactant solution to stabilize the emulsion and allow the determination of its droplet size distribution with the use of microscopy later on ground.

The dynamic behaviour and stability of produced emulsions are investigated inside the experimental cells under

Fig. 4 **a** The cell case supporting five identical experimental cells, **b** Carrier motion that allows the use of a different experimental cell in each parabola of a 5-parabolas sequence and **c** The experimental cell



low gravity conditions by means of advanced optical and electrical diagnostics. The optical diagnostics unit has been designed and constructed to incorporate two cameras (an advanced high speed camera and a conventional DSLR one) combined with a cube beam splitter, which enables simultaneous optical recording of the emulsion behaviour by these two cameras, as well as LED backlight to provide the necessary illumination (Fig. 5). The Photron Multi FAST-CAM high speed camera (up to 750.000 fps, 1280 x 1024 pixels) is used to: a) Monitor the breakup of droplets and study their shape evolution during emulsification process and b) Investigate droplet-droplet interactions (coalescence and aggregation) and determine kinetic parameters and characteristic times of droplets collision after the completion of emulsification process. The CANON EOS 70D digital camera (20MP), combined with CANON EF Macro USM lens (100mm f/2.8) and six CANON extension rings

(total length 130mm) to increase image resolution, is utilized to capture successive oil droplets images of the produced emulsion. Image analysis with the custom software BubbleSEdit, which is capable of detecting even strongly

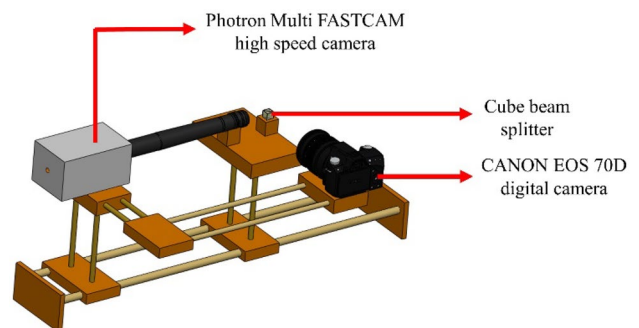


Fig. 5 The optical diagnostics unit of the 1st experiment rack

overlapping droplets under varying illumination conditions, provide the evolution of droplet size distribution with time and gravity (Zabulis et al. 2007). PFV4 and EOS Utility software (installed in different laptops) are used to control the high speed and the DSLR camera, respectively. Both cameras as well as the beam splitter are supported by custom-made metallic holders, which allow fine tuning of the supporting item position in the X-Y-Z axis using proper micro-manipulators.

The EU patented I-VED electrical diagnostic (*EP 3 005 942 A1, 2016*) is employed to estimate oil volumetric fraction inside the experimental cell and, thus, enables to investigate its evolution as a function of time and gravity after the end of emulsification. Furthermore, it allows to validate droplet size distributions derived from optical measurements. I-VED has been developed in the framework of an ESA GSTP Project (Contract No.: 4000101764, 2005-2015) for the detection of bubbles in astronauts' bloodstream during Decompression Sickness and offers 2-3 orders of magnitude higher sensitivity and accuracy compared to other conventional electrical techniques. So far, it has been successfully tested in different two-phase systems, as well as in a few in-vivo studies (Evgenidis and Karapantsios 2015; Gkotsis et al. 2019; Gkotsis et al. 2020; Oikonomidou et al. 2018; Oikonomidou et al. 2019; Vlachou et al. 2020; Tzevelekos et al. 2021; Evgenidis and Karapantsios 2022; Evgenidis et al. 2023). Here, a dedicated I-VED version has been designed and implemented to fulfill the requirements of the system under study and to be incorporated in the experimental device of the Parabolic Flights (Fig. 6). I-VED operation is only briefly presented below, since it has been previously described analytically by the authors (Evgenidis and Karapantsios 2015; Gkotsis et al. 2019; Gkotsis et al. 2020; Oikonomidou et al. 2018; Oikonomidou et al. 2019; Vlachou et al. 2020). I-VED performs electrical impedance measurements through the two rod electrodes (Fig. 4c), which are in contact with the emulsion under study. A Function/Arbitrary Waveform Generator (DG1022, RIGOL) produces a sinusoidal voltage signal with an amplitude of 2 V_{p-p} and a frequency of 25 kHz that excites electrically the two-phase system and, then, a 20-bit data acquisition card (ZOOM UAC-2 / USB 3.0 Audio Converter) records the electrical signal with a sampling frequency of 192 kHz. Obtained signal is digitally processed and filtered by a custom Matlab routine, while the final output of data reduction is an electrical impedance time-series which is transformed to oil volumetric fraction time-series employing the appropriate model (e.g Maxwell or Bruggeman) (Evgenidis and Karapantsios 2015).

Each of the three laptops which are secured on the top of the 1st rack performs a specific function during the experiment: 1) Programming the Photron Multi FASTCAM (shutter speed, frame rate, ISO, recording duration) to record high

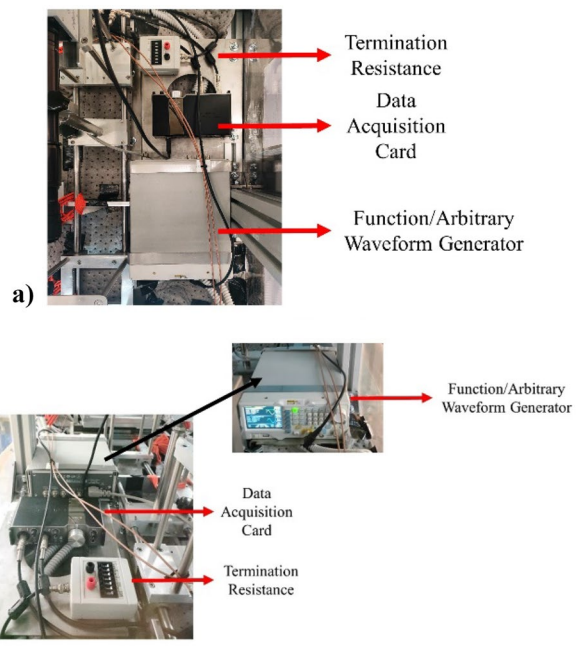


Fig. 6 The electrical diagnostics unit of the 1st experiment rack; **a** top view, **b** side view

speed videos, 2) Tuning I-VED settings (signal frequency and amplitude, recording duration) and conducting electrical impedance measurements, and 3) Programming the stepper motor (pulsation stroke frequency and emulsification duration) and the CANON EOS 70D camera (aperture, shutter speed, ISO, time interval of successive shots) to take still images of oil droplets.

2nd Rack

The 2nd rack of the device includes solely the storage unit that secures six cases supporting five experimental cells each (thirty experimental cells in total) (Fig. 7).

Baseplate

The baseplate is used to secure the electrical control panel of the device and the processor of the high speed camera by means of Rexroth Bosch[®] brackets and straps (Fig. 8).

Experimental Procedure to Follow During Parabolic Flights

Each ESA Parabolic Flight Campaign (PFC) includes 3 days of experiments under micro-gravity conditions, which are performed onboard the Novespace aircraft. The aircraft performs 30 parabolas each day, so 30 experiments

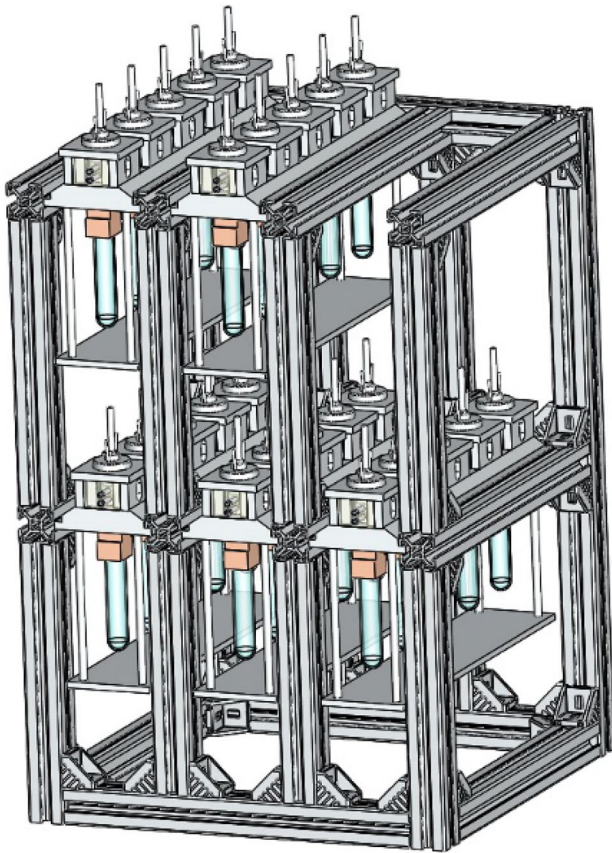


Fig. 7 The 2nd rack of the experimental device that includes solely the storage unit for the experimental cells

are conducted every single day and 90 experiments in total (3 days x 30 micro-gravity experiments).

All the 30 experimental cells are cleaned and filled before each experimental day of the PFC. Proper aqueous solutions are prepared and, since the lid of the cell (with the piston on it) is already in place, the pre-defined volume of the aqueous phase is added into the cell through the first port while the organic phase is added next through the second port. The

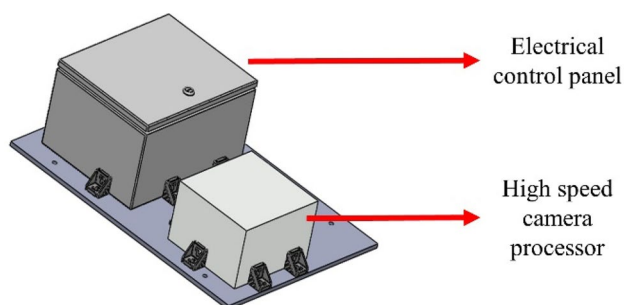


Fig. 8 The baseplate of the experimental device

insertion of the two liquids takes place using syringes. At the end, both ports are closed by caps and the cell is ready for pulsation. Moreover, ~2mL of a dense surfactant solution are added in the PP tube at the bottom part of each experimental cell to inhibit droplets coalescence of the collected emulsion at the end of each experiment, allowing its investigation by means of optical microscopy later on ground.

At the beginning of each experimental day, all the cells are placed and secured in the storage unit on-board the aircraft. After the take-off and before the first parabola, all the electrical devices (electrical control panel, cameras, laptops function/arbitrary waveform generator and data acquisition card) are switched on. The 1st cell case is placed to the emulsification unit and two different connections are made: a) the piston axis of the 1st experimental cell to the stepper motor and b) I-VED electrodes to the 1st experimental cell.

The parabolic maneuver total duration is ~70 s and the length of weightlessness is ~22 s. The maneuver includes three different phases: a) entry phase (vertical load factor of 1.8g / ~24 s), b) injection phase (vertical load factor goes from 1.8g to 0g / ~22 s) and c) exit phase (symmetrical with the entry phase / ~20 s). The emulsification process takes place normally during 0g conditions, but it may start earlier (i.e. in entry phase, 1.8g) in the case it needs to last too long (more than 10s). I-VED performs electrical measurements for the total duration of the maneuver, the Photron Multi FASTCAM records video for a few seconds (during emulsification but mainly after its completion to study droplets' interactions) and the CANON EOS 70D is programmed to take still images of oil droplets every 5 s (starting during emulsification and ending in the exit phase of the maneuver).

In the ninety seconds break between the 1st and the 2nd parabola (~1g gravity conditions), the valve at the bottom of the 1st cell is opened and the emulsion drains into the PP tube where it is stabilized in the presence of proper surfactant solution. Then, the piston axis and electrodes are disconnected from the 1st cell, the case is moving to the 2nd cell and its piston axis is connected with the stepper motor while I-VED electrodes are connected to this cell as well. This procedure is followed for the next experiments and at the end of the first set of five parabolas, the first case is replaced by another one consisting of five more experimental cells. In total, six cases will be used in each day of the campaign aiming to conduct thirty experiments.

Test Liquids and Parameters to Examine During Parabolic Flights

As already mentioned, the emulsions are heterogeneous systems consisting of two phases, the aqueous and the organic one. The main components for the preparation of emulsions to be examined under micro-gravity conditions during parabolic flights are the following: millipore water (0.05 μ S/cm,

Direct-Q[®] 3UV), dodecane (Sigma-Aldrich, purity $\geq 99\%$) or MCT oil (IOI Oleo Chemical) and sodium dodecyl sulfate (SDS; Sigma-Aldrich, water soluble, anionic surfactant, purity $\geq 98.5\%$, CMC: 0.008 M) or Nikkol BL-21 (Nikko Chemicals, water soluble, nonionic surfactant, CMC: 2×10^{-4} M) surfactant as emulsifier. Dodecane and SDS are commonly used in emulsions studied in different applications on ground, while MCT oil and Nikkol BL-21 are used in FOAM-C experiment on-board the ISS. Aqueous solutions of SDS or Nikkol BL-21 surfactant are employed as the aqueous phase and dodecane or MCT oil are applied as the organic phase of emulsions to be tested onboard the aircraft. The four parameters to be examined during the study of emulsion dynamic behavior and stability under microgravity conditions are: a) surfactant (SDS or Nikkol BL-21) concentration (from 0 to 1 CMC), b) emulsification duration (t_n) (ranging from 0.6 to 20 s), c) oil volume fraction (φ) (from 0.01 to 0.3) and d) pulsation stroke frequency (f) (from 5 to 15 Hz). It is mentioned that abovementioned values may change during the experiments based on the obtained results, while a number of parabolas will be used for repeatability tests.

Preliminary (Ground) Experiments and Respective Results

To assess and confirm the functionality of the experimental setup in view of the forthcoming parabolic flights, we conducted a number of preliminary on-ground experiments. Tests were performed with a conventional oil in water emulsion consisting of an aqueous solution of SDS ($C_{SDS} = 1$ CMC) as the aqueous phase and dodecane as the organic phase, while experimental parameters were the following: pulsation stroke frequency, emulsification duration and oil volume fraction. I-VED electrical measurements were conducted both during the emulsification and after its completion for 50 seconds. Photron Multi FASTCAM high speed camera was used to monitor droplets motion and coalescence events for 20 seconds after the end of the emulsification as well. Then, the bottom valve of the experimental cell was opened and the emulsion was drained into the PP tube that contained an aqueous solution of 5% w/w SDS to inhibit droplets coalescence. The diluted emulsion was mildly hand shaken to become homogeneous and, then, a sample of 0.2 mL was placed on a microscope slide with a cover glass above.

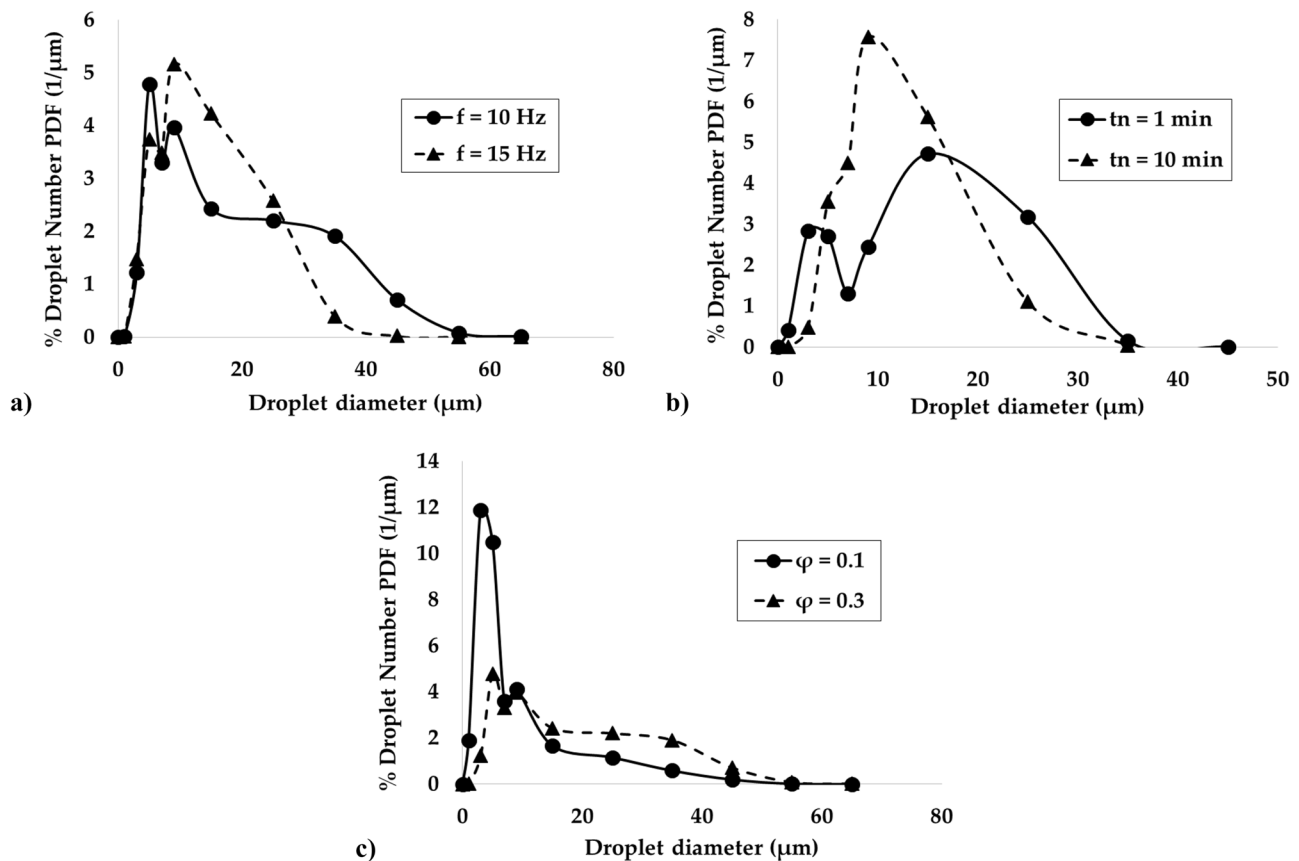
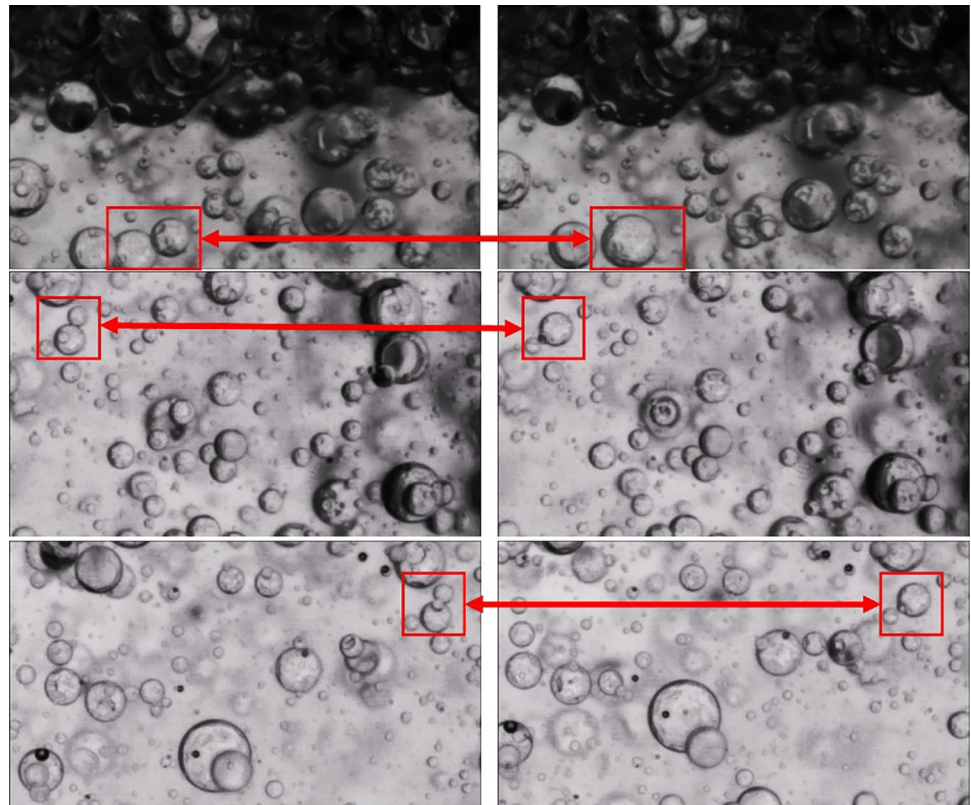


Fig. 9 Effect of **a** pulsation stroke frequency, f ($t_n = 2$ min, $\varphi = 0.3$, $C_{SDS} = 1$ CMC); **b** emulsification time, t_n ($f = 15$ Hz, $\varphi = 0.3$, $C_{SDS} = 1$ CMC) and **c** oil volume fraction, φ ($t_n = 2$ min, $f = 10$ Hz, $C_{SDS} = 1$ CMC) on droplet size probability density function

Fig. 10 Indicative coalescence events in the aqueous phase



A transmitted light optical microscopy (Axiostar plus, Zeiss) combined with a Canon PowerShot A640 video camera was used to obtain high resolution (10 megapixels) images of oil droplets. These images were finally analyzed with BubbleSEdit software to determine droplet size distribution (Zabulis et al. 2007). In general, there is a critical number of droplets that must be measured so as to ensure statistical accuracy. In the present study, a population of at least 1500 droplets is measured for the determination of droplet size distribution (Caserta et al. 2004; Caserta et al. 2005).

Indicative droplet size distributions are presented in Fig. 9. The distributions are presented in terms of probability density function (PDF) which implies that the integral of the area under each curve is 100%. The first examined parameter is the pulsation stroke frequency, f . Two f values are compared, 10 and 15 Hz, for emulsions produced with emulsification time (t_n) of 2 minutes (Fig. 9a). Two different t_n values are tested next, 1 and 10 minutes, for emulsions produced with an f value of 15 Hz (Fig. 9b). In both cases the oil volume fraction (φ) applied is 0.3. Finally, the effect of oil volume fraction is examined for emulsions produced with $f = 10$ Hz and $t_n = 2$ minutes (Fig. 9c). In general, the droplet size distribution becomes narrower (and accordingly sharper) towards smaller sizes, which means that the produced emulsions are more stable, when: a) the oil volume fraction reduces and b) the emulsification time and stroke frequency increase.

During on-ground experiments, water phase separation takes place immediately after the end of emulsification. This refers to the separation between the creamy phase (high oil volume fraction) and the aqueous phase (low oil volume fraction). It must be noted that both phases (creamy and aqueous) are both emulsions but include very different oil proportions. On earth, gravity triggers the rapid separation of aqueous phase from creamy phase and, as expected, the large droplets move faster to the top of the cell than the smaller ones. By analyzing the video taken using the Photron Multi FASTCAM high speed camera, it is concluded that the majority of coalescence events is observed on the bottom part of the piston plate (creamy phase). The oil droplets come in close contact with each other, pressure is exerted due to buoyancy effect, and the coalescence phenomenon takes place. As far as the aqueous phase is concerned, the residual motion of piston periodical movement leads to oil droplets collisions and consequently to coalescence events. When two oil droplets are in contact, the liquid film between them ruptures and the coalesced droplet instantaneously obtains a spherical shape. Isolated coalescence events in the aqueous phase are shown in Fig 10. In all three cases the two droplets which merge to a single droplet seem to have different sizes but this is not considered as requirement for the coalescence phenomenon to take place. Two oil droplets of the same size can also coalesce. Furthermore, droplet coalescence may happen in different directions (vertically,

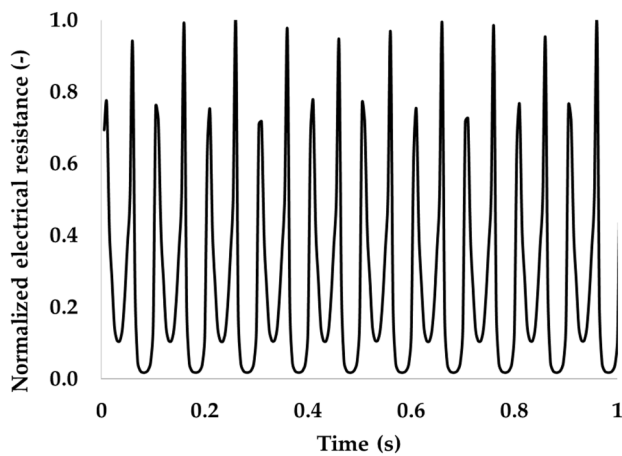


Fig. 11 Evolution of emulsion electrical resistance during the periodical movement of the piston with a frequency of 10 Hz for 1 s

horizontally, and diagonally), as has been also noticed for the case of coalesced bubbles (Sielaff et al. 2014).

Finally, I-VED measurements capture with high sensitivity the variation of emulsion electrical resistance during both emulsification and phase separation. Fig. 11 presents the evolution of electrical resistance during the periodical movement of the piston with a frequency of 10 Hz for 1 s. As shown, ten intense signal peaks can be clearly noticed in 1 s, corresponding to the applied pulsation stroke frequency.

Figure 12 compares three I-VED signals during phase separation of emulsions with varying oil volume fraction φ (0.01, 0.1, and 0.2). Electrical resistance decreases progressively during phase separation since oil droplets (non-conductive phase) rise in the cell due to buoyancy and the measuring volume between the electrodes contains more and more the aqueous (conductive) phase. At the beginning of

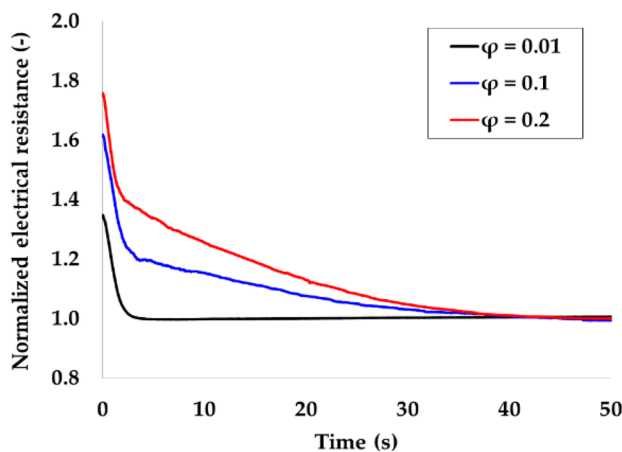


Fig. 12 Normalized electrical resistance as a function of time during phase separation of emulsions with different oil volume fraction ($t_n = 30$ s, $f = 10$ Hz, $C_{SDS} = 1$ CMC)


phase separation, the electrical resistance gets the highest value for the largest oil volume fraction (0.2); at the end of the separation, however, the three signals converge because the measured electrical resistance concerns solely the aqueous phase and is independent of the oil volume fraction.

Conclusions

This work presents the design, development and preliminary testing of a new experimental device to be used in the forthcoming ESA parabolic flights for the assessment of emulsions' dynamic behavior and stability under low gravity conditions. Such conditions allow to get rid of the gravity driven emulsion destabilization mechanisms (sedimentation and creaming) and, therefore, to study in-depth solely the interface driven mechanisms (droplets' coalescence and aggregation). The device consists of three parts, two experiment racks and one separate baseplate. The 1st rack incorporates the novel miniature pulsating emulsification device used on-ground by Chondrou et al. (Chondrou et al. 2020, 2021), as well as advanced electrical and optical diagnostics to study the produced oil in water emulsions in custom experimental cells. An optical diagnostics unit is furnished with a high speed camera (up to 750.000 fps) to monitor droplets' breakup and droplet-droplet interactions, as well as a high resolution DSLR camera (20MP) combined with a 100 mm macro lens to determine droplet size distribution. On the other hand, the EU patented I-VED electrical impedance spectroscopy technique (*EP 3 005 942 A1, 2016*) is employed to monitor the evolution of oil volumetric fraction as a function of time and gravity inside the experimental cell. The 2nd rack is used as a storage unit for thirty experimental cells and the baseplate is used to secure the electrical control panel of the device and the processor of the high-speed camera. The implementation of the experimental device complies with ESA technical requirements and safety regulations, while a number of experiments on-ground with a conventional oil in water emulsion validates it by a technical and functional point of view. Specifically, it is demonstrated that: a) I-VED signals carry useful information on phase separation of emulsions, b) Droplets' coalescence phenomenon is successfully captured by the high speed camera and c) Droplet size distribution is shifted to smaller sizes and becomes narrower with the increase of the pulsation duration/stroke frequency during emulsification and decrease of oil volume fraction. Finally, the implementation of a non-invasive spectroscopic technique, Diffusing Wave Spectroscopy (DWS), to investigate the structure and dynamics of the generated emulsions should be considered for future development of the experimental device (Orsi et al. 2019).

Acknowledgements Authors are really thankful to K. Noula and D. Komitis for their help in high speed imaging.

Authors' Contributions Angeliki P. Chondrou: Conceptualization, Methodology, Writing – original draft preparation. Sotiris P. Evgenidis: Conceptualization, Methodology, Writing – original draft preparation. Konstantinos A. Zacharias: Methodology. Margaritis Kostoglou: Conceptualization, Methodology, Writing – review and editing. Supervision. Thodoris D. Karapantsios: Conceptualization, Methodology, Writing – review and editing, Funding acquisition, Supervision.

Funding This study was funded by  PRODEX Project: Dynamics of Emulsion Droplet Interactions in Low Gravity Conditions, Low-G-Emulsion – Contract No.: 4000132920. The view expressed herein can in no way be taken to reflect the official opinion of the European Space Agency.

Availability of Data and Material The datasets generated during and/or analyzed during the current study are available from the corresponding author on reasonable request.

Declarations

Ethics Approval The authors confirm that this work is original and has not been published elsewhere nor is it currently under consideration for publication elsewhere.

Consent to Participate Not applicable.

Consent for Publication Not applicable.

Conflicts of Interest All authors certify that they have no affiliations with or involvement in any organization or entity with any financial interest or non-financial interest in the subject matter or materials discussed in this manuscript.

References

- Akbari, S., Hamid Nour, A.: Emulsion types, stability mechanisms and rheology: A review. *Int. J. Innov. Res. Sci. Stud.* **1**(1), 14–21 (2018)
- Born, P., Braibanti, M., Christofolini, L., Cohen-Addad, A., Durian, D.J., Egelhaaf, S.U., Escobedo-Sanchez, M.A., Hohler, R., Karapantsios, T.D., Langevin, D., Liggieri, L., Pasquet, M., Rio, E., Salonen, A., Schroter, M., Sperl, M., Sutterlin, R., Zuccolotto-Bernez, A.B.: Soft matter dynamics: A versatile microgravity platform to study dynamics in soft matter. *Rev. Sci. Instrum.* **92**, 124503 (2021)
- Caserta, S., Simeone, M., Guido, S.: Evolution of drop size distribution of polymer blends under shear flow by optical sectioning. *Rheol. Acta* **43**, 491–501 (2004)
- Caserta, S., Sabetta, L., Simeone, M., Guido, S.: Shear-induced coalescence in aqueous biopolymer mixtures. *Chem. Engin. Sci.* **60**, 1019–1027 (2005)
- Chappat, M.: Some applications of emulsions. *Colloids Surf A: Physicochem. Eng.* **91**, 57–77 (1994)
- Chondrou, A.P., Evgenidis, S.P., Kostoglou, M., Karapantsios, T.D.: An innovative Miniature Pulsating Emulsification Device: Flow Characterization and Measurement of Emulsion Stability. *Colloids Interfaces* **4**(1), 7 (2020)
- Chondrou, A.P., Karapantsios, T.D., Kostoglou, M.: Effect of width/height of the gap between piston and wall on the performance of a novel small volume emulsification device. *Colloids Surf. A: Physicochem. Eng.* **622**, 126702 (2021)
- Evgenidis, S.P., Karapantsios, T.D.: Effect of bubble size on void fraction fluctuations in dispersed bubble flows. *Int. J. Multiph. Flow* **75**, 163–173 (2015)
- Evgenidis, S.P., Karapantsios, T.D.: Pulsatile gas-liquid flow resembling Decompression Sickness: Computational Fluid Dynamics simulation and experimental validation. *International Maritime Health* **73**(4), 189–198 (2022)
- Evgenidis, S., Chondrou, A., Karapantsios, T.: A new phantom that simulates electrically a human blood vessel surrounded by tissues: Development and validation against in-vivo measurements. *Ann. Biomed. Eng.* **6**, 1284–1295 (2023)
- Gkotsis, P.K., Evgenidis, S.P., Karapantsios, T.D.: Influence of Newtonian and non-Newtonian fluid behaviour on void fraction and bubble size for a gas-liquid flow of sub-millimeter bubbles at low void fractions. *Exp. Therm. Fluid Sci.* **109**, 109912 (2019)
- Gkotsis, P.K., Evgenidis, S.P., Karapantsios, T.D.: Associating void fraction signals with bubble clusters features in co-current, upward gas-liquid flow of a non-Newtonian liquid. *Int. J. Multiph. Flow* **131**, 103297 (2020)
- Guido, S., Simeone, M.: Binary collision of drops in simple shear flow by computer-assisted video optical microscopy. *J. Fluid Mech.* **357**, 1–20 (1998)
- Leal-Calderon, F., Schmitt, V., Bibette, J.: *Emulsion Science: Basic Principles* 2nd Ed., Springer: City, USA (2007)
- Liu, X., Chengyao, W., Zhao, Y., Chen, Y.: Shear-driven two colliding motions of binary double emulsion droplets. *J. Heat Mass Transf.* **121**, 377–389 (2018)
- Lorusso, V., Orsi, D., Salerni, F., Liggieri, L., Ravera, F., McMillin, R., Ferri, J., Christofolini, L.: Recent developments in emulsion characterization: Diffusing Wave Spectroscopy beyond average values. *Adv. Colloid Interface Sci.* **288**, 102341 (2021)
- McClements, D.J.: *Food Emulsions: Principles, Practices and Techniques*, 2nd edn. CRC Press, Florida (2005)
- Oikonomidou, O., Evgenidis, S.P., Kostoglou, M., Karapantsios, T.D.: Degassing of a pressurized liquid saturated with dissolved gas when injected to a low pressure liquid pool. *Exp. Therm. Fluid Sci.* **96**, 347–357 (2018)
- Oikonomidou, O., Evgenidis, S.P., Schwarz, C.J., van Loon, J.J.W.A., Kostoglou, M., Karapantsios, T.D.: Degassing of a decompressed flowing liquid under hypergravity conditions. *Int. J. Multiph. Flow* **115**, 126–136 (2019)
- Orsi, D., Salerni, F., Macaluso, E., Santini, E., Ravera, F., Liggieri, L., Christofolini, L.: Diffusing wave spectroscopy for investigating emulsions: I. Instrumental aspects. *Colloids Surf A: Physicochem. Eng.* **580**, 123574 (2019)
- Rosen, M.J.: *Surfactants and interfacial phenomena* 3rd Ed., John Wiley & Sons Inc.: New Jersey, NJ, USA (2004)
- Schramm, L.L.: *Emulsions, Foams and Suspensions. Fundamentals and Applications*. Wiley-VCH Verlag GmbH & Co. KGaA, Weinheim, Germany (2005)
- Sielaff, A., Dietl, J., Herbert, S., Stephan, P.: The influence of system pressure on bubble coalescence in nucleate boiling. *Heat Transfer Eng.* **35**(5), 420–429 (2014)
- Tadros, T.F.: *Emulsion Formation and Stability*, 1st edn. Wiley-VCH Verlag GmbH & Co. KGaA, Weinheim, Germany (2013)
- Tzevelekos, W., Galand, Q., Evgenidis, S., Zacharias, K., Karapantsios, T., Vaerenbergh, S.: High-resolution concentration measurement in water/n-butanol binary system by means of high-frequency electrical impedance method. *Exp. Therm. Fluid Sci.* **126**, 110399 (2021)
- Varka, E.M., Karapantsios, T.D.: Global versus local dynamics during destabilization of eco-friendly cosmetic emulsions. *Colloids Surf A: Physicochem. Eng.* **391**, 195–200 (2011)

- Vlachou, M.C., Zacharias, K.A., Kostoglou, M., Karapantsios, T.D.: Droplet size distributions derived from evolution of oil fraction during phase separation of oil-in-water emulsions tracked by electrical impedance spectroscopy. *Colloids Surf. A: Physicochem. Eng.* **586**, 124292 (2020)
- Zabulis, X., Papara, M., Chatziargyriou, A., Karapantsios, T.D.: Detection of densely dispersed spherical bubbles in digital images based on a template matching technique. Application to wet foams. *Colloids Surf A: Physicochem. Eng.* **309**(1-3), 96-106 (2007)

Publisher's Note Springer Nature remains neutral with regard to jurisdictional claims in published maps and institutional affiliations.

Springer Nature or its licensor (e.g. a society or other partner) holds exclusive rights to this article under a publishing agreement with the author(s) or other rightsholder(s); author self-archiving of the accepted manuscript version of this article is solely governed by the terms of such publishing agreement and applicable law.